Desalination and Water Treatment
www.deswater.com

doi: 10.1080/19443994.2015.1085447

57 (2016) 17483–17493
August

Taylor & Francis
Taylor & Francis Group

Coke/Fe_3O_4 nanoparticle composites: synthesis, characterization and adsorption behaviour towards organic dyes

S.K. Giri[a], P. Sahoo[a], R. Das[b], N. Das[a,c,*]

[a]*Department of Chemistry, North Orissa University, Baripada 757 001, Odisha, India,*
emails: sumankumargiri@gmail.com (S.K. Giri), pranakr@rediffmail.com (P. Sahoo), Fax: +91 671 2510304
emails: dasnn64@rediffmail.com, dasn@ravenshawuniversity.ac.in (N. Das)
[b]*Department of Chemistry, R.D. Women's (A) College, Bhubaneswar 75100, India, email: dasrita66@rediffmail.com*
[c]*Department of Chemistry, Ravenshaw University, Cuttack 753003, Odisha, India*

Received 22 January 2015; Accepted 14 August 2015

ABSTRACT

Coke/Fe_3O_4 composites using varying sizes of coke samples derived from hard/soft coking coals blending with Fe_3O_4 nanoparticles, generated *in situ* or added *ex situ*, were prepared and characterized by several physicochemical methods. Powder X-ray diffraction, UV–vis–DRS and SEM–EDX confirmed the presence of both coke and magnetite nanoparticles (MNP) in the composite samples, while transmission electron microscopy revealed nearly a uniform distribution of MNP on coke. The obtained composites combined the features of coke and Fe_3O_4 nanoparticles were efficient and fast in the removal of several aqueous organic dyes and the adsorption efficiency was mainly depended on the solution pH, initial dye concentration and adsorbate/adsorbent ratio. Batch equilibrium adsorption results of congo red (CR) and methylene blue (MB) were best described by the Freundlich isotherm model. In comparison, the desorption of adsorbed dyes on composites was much easier in the case of anionic dyes like CR than cationic one (MB). The present study showed that the as-prepared coke/Fe_3O_4 composites could be utilized as a low-cost efficient and magnetically separable adsorbent for the environmental remediation.

Keywords: Coke; Magnetite nanoparticles; Coke/Fe_3O_4 composite; Nanoadsorbent; Organic dyes

1. Introduction

Adsorption is one of the most widely adopted methods in the treatment of different contaminated waters due to its simplicity, high efficiency and easy operational conditions in addition to the availability of a wide range of synthetic and naturally occurring adsorbents [1–5]. Among various adsorbents used in the treatment of contaminated waters, the carbonaceous materials including activated carbons/charcoals (ACs) have been most extensively used owing to their relatively high surface area, porosity and chemical inertness [6–9]. One of the major problems associated with the use of ACs in adsorption processes is their separation from the treated water for regeneration and further use. The conventional separation procedures like filtration and centrifugation are not very much effective, especially when the particle sizes of ACs are very small which extends up to nanometric range and used alone as the adsorbent. It could lead to the blockage of filters or the loss of solid adsorbent particles. In

*Corresponding author.

1944-3994/1944-3986 © 2015 Balaban Desalination Publications. All rights reserved.

addition, the problems of dispersion and turbidity in the system are also encountered in case of very small particle-sized ACs which limit their large-scale applications as adsorbents. In order to overcome the separation problem of small particle-sized adsorbents, a great deal of research has been devoted in recent years on the fabrication of magnetically separable adsorbents (neat/composites) for their effective use in the treatment of contaminated water [10–15]. In such cases, the sorbents could be easily separated from solution after the sorption process by magnetic assistance for further use.

Several methods such as high energy milling [16], reducing [17], impregnation [18] and chemical coprecipitation [19] have been adopted to develop the magnetic iron–AC composites for their possible application as adsorbents. In this regard, the fabrication of adsorbents containing ACs/graphene with iron-based magnetic component like magnetite nanoparticles (MNP) and their use for the removal of organic contaminants including dyes have been a subject of several recent investigations [18,20–22]. The presence of MNP in the adsorbents not only facilitates their separation, but also enhances the rate of adsorption significantly.

Coke, another important carbonaceous material derived from coal by removing moisture and other volatile matters, is mostly used in metallurgical processes. The overall properties of the coke largely depend on the nature of coals used as the starting material, ratio of different coals and preparation method. Although the adsorption properties of ACs have been exhaustively studied for different adsorbates, the adsorption efficiency of coke has been sparsely studied [23,24]. Moreover, the adsorption property of coke/MNP composites is yet to be explored.

In sequel to our study on the synthesis of coke samples from coking coals and their adsorption efficiency for the removal of phenols from effluents of coke oven plant and MNP from waste iron ore tailing (IOT) for different applications [11a,25], the present study aimed at synthesis and characterizations of coke/MNP composite samples for the adsorptive removal of aqueous organic dyes.

2. Materials and methods

2.1. Materials

IOTs with relatively high iron content (≈39.01%) were used as one of the starting materials for the synthesis of MNP. $FeSO_4{\cdot}7H_2O$, HCl, NaOH, liquid ammonia (Merck) and sodium dodecyl sulphonate (SDS) (Sd-fines) were used for the digestion of IOT, and synthesis of MNP and coke/Fe_3O_4 composites. Methylene blue (MB) and congo red (CR) were used as received from Qualigens and BDH, respectively, for adsorption experiments. All other chemicals used were of analytical grade. Coke samples of different sizes (named as C-297, C-149 and C-62 for samples of 297, 149 and 62 μ (micron) particle sizes, respectively) prepared from a mixture of hard/soft-coking coals were used for the synthesis of coke/Fe_3O_4 composites.

2.2. Synthesis of neat MNP (Fe_3O_4) and coke/Fe_3O_4 nanoparticle composites

MNP was synthesized using recovered ferric iron from IOT as one of the starting materials following the procedure described previously [11a] and stored in deoxygenated water. The solid content, i.e. dispersed MNP was found to be 17.83 mg mL^{-1}. Coke/Fe_3O_4 composites, using coke powder of different sizes as mentioned above, were prepared by both *ex situ* and *in situ* methods. In the case of *ex situ* method, a desired amount of coke samples was sonicated (50 MHz) for 1 h with a fixed amount of previously synthesized MNP to yield the coke/MNP composites. In the case of *in situ* method, Fe^{II}/Fe^{III} solution in appropriate ratio was treated with a desired amount of coke of different sizes and the precipitation was effected by the addition of NaOH (1.0 M) solution under N_2 atmosphere under stirring condition. Six coke/Fe_3O_4 composites (Table 1) were prepared using coke samples of three different sizes and hereafter referred as In-297, In-149, In-62, Ex-297, Ex-149 and Ex-62, where In and Ex stand for *in situ* and *ex situ*, while numbers indicate the size of coke. The resulted coke/Fe_3O_4 nanoparticle composites were separated by centrifugation, dried in vacuum and stored in air-tight bottle for characterizations and used as adsorbents.

Table 1
Composition and surface area values of neat samples and coke/MNP composites

Sample	Coke/Fe_3O_4 (wt%)	Surface area (m^2/g)
In-297	33.6/65.4	17.32
Ex-297	31.9/66.1	13.54
In-149	59.5/40.6	27.32
Ex-149	56.3/42.8	25.73
In-62	64.7/33.3	34.20
Ex-62	61.3/35.7	31.89
C-297	–	7.23
C-149	–	11.39
C-62	–	21.28
Neat MNP	–	25.12

2.3. Physicochemical characterizations

The major constituents of neat MNP and coke/Fe_3O_4 nanoparticle composites were determined by conventional wet chemical analysis of Fe^{III}/Fe^{II}, while AAS (Perkin Elmer, 3100) or ICP-OES (Perkin Elmer, 4300) was used to analyse the minor constituents (Mn, Ni, Cu, Si, Al, Ti, Mg and Ca) in MNP. Powder X-ray diffraction (PXRD) patterns were recorded on a Rigaku Miniflex II at a scanning speed of $1.2^\circ\,min^{-1}$ using nickel-filtered Cu–Kα radiation (30 kV, 15 mA). UV–vis–diffuse reflectance spectra (UV–vis-DRS) were recorded on a Shimadzu, UV-2400 spectrophotometer using $BaSO_4$ as a reference. The surface area of different samples was determined by BET method using Smart Sorb 92/93 surface area analyser. Magnetic measurements were made using a vibrating sample magnetometer (Lakeshore 7410) under an applied magnetic field (+20,000 to -20,000 G) at room temperature. The morphology observed with a JEOL JSM-6390 LV scanning electron micrographs operated at 15 kV. The size and distribution of neat MNP or coke/Fe_3O_4 composites were studied by a transmission electron microscope (TEM2100, JEOL) operated at 200 kV. The point of zero charge (pH_{pzc}) of different samples was determined by batch acid–base titration, described previously [11a]. As coke/Fe_3O_4 samples (In-62 and Ex-62) exhibit highest surface area as well as maximum dye adsorption, detailed characterizations of these two samples were carried out in this study.

2.4. Adsorption and desorption studies

The adsorption efficiency of coke/Fe_3O_4 composites was assessed by batch equilibrium technique using both cationic (MB) and anionic (CR) dyes. The temperature and shaking speed for all the adsorption experiments were kept constant at 30.0 ± 0.2°C and 120 rpm, respectively, using a thermostated water bath shaker. Preliminary studies indicate that the adsorption equilibrium was relatively fast and attained within 2–5 min, and no further adsorption of MB or CR on coke/Fe_3O_4 composite was observed on further shaking up to 30 min. Typically, 50 ml of dye solutions with different MB or CR (10–100 mg L^{-1}) concentrations was shaken with varying amounts of neat MNP or coke/Fe_3O_4 composites (1.0–4.0 g L^{-1}) for 5–10 min. The pH of the solution was adjusted to desired values using dilute HCl/NaOH before the addition of adsorbent (MB; pH ≈ 9 or CR; pH ≈ 6). The concentrations of residual MB or CR, after magnetic separation of coke/Fe_3O_4 composite, were computed by measuring the absorbance at λ_{max} (665 and 495 nm for MB and CR, respectively) using UV–vis spectrophotometer (Systronics, 2204). The amount of dye adsorbed (q_e) and efficiency (%) of adsorbent were calculated using the following equations:

$$q_e = (C_i - C_e)V/m \quad (1)$$

$$\text{Dye removal efficiency } (\%) = [(C_i - C_e)/C_i] \times 100 \quad (2)$$

where q_e, q_i, C_i, C_e, V and m represent the amount of dye adsorbed on the adsorbents (mg g^{-1}), the initial dye concentration (mg L^{-1}), the final concentration (mg L^{-1}), volume of the dye solution (L) and the amount of coke/Fe_3O_4 composite (g), respectively. The adsorption data were fitted to the Langmuir and Freundlich models to derive various adsorption parameters.

For desorption of adsorbed MB/CR on coke/Fe_3O_4 composites, the MB-loaded sample was dispersed into the methanolic solution of acetic acid (2–12 v/v %) or CR-loaded coke/Fe_3O_4 nanoparticle composites were dispersed in an aqueous medium maintained at different pH and stirred for a predetermined time of 5 min. The concentrations of MB/CR desorbed, after the magnetic separation of coke/Fe_3O_4 composites, were determined spectrophotometrically as described above.

3. Results and discussion

3.1. Characterizations of neat MNP and coke/Fe_3O_4 composites

The total iron contents in MNP or coke/Fe_3O_4 composites, calculated using the analytical results of Fe^{II}/Fe^{III}, were found very close to the theoretical value (72.36%) indicating the purity of MNP. Further, the presence of minor constituents (Mn, Ni, Cu, Si, Al, Ti, Mg and Ca) in MNP was collectively found less than 100 ppm indicating MNPs prepared using naturally occurring IOT as one of the starting materials was relatively pure.

The XRD patterns of MNP and representative coke/Fe_3O_4 composites are presented in Fig. 1. As evident, the peaks of neat MNP (Fig. 1(a)) matched with face-centred Fe_3O_4 (JCPDS file No. 19-0629). The composite samples In-62 and Ex-62 also showed (Fig. 1(b) and (c)) the characteristic peaks of Fe_3O_4 with lower intensity besides an additional peak at $2\theta = 26.4^\circ$ due to coke, indicating the coexistence of MNPs and coke in the composite. The mean size of Fe_3O_4 crystallites in neat MNP, In-62 and Ex-62, estimated using Debye–Scherrer's equation ($D = K\lambda/\beta\cos\theta$), was

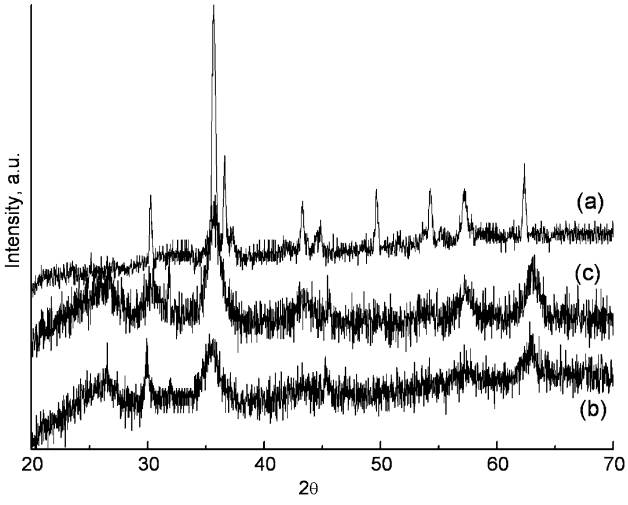

Fig. 1. Powder XRD patterns of (a) neat MNP, (b) In-62 and (c) Ex-62.

found to be 8.4, 7.6 and 7.9 nm, respectively. The estimated crystallite size of value MNP was very close to that obtained from TEM (see later) indicating that each MNP particle was a single crystal.

The UV–vis–DRS of MNP (Fig. 2(a)) and representative coke/Fe_3O_4 composites (In-62 and Ex-62, Fig. 2(b) and (c)) showed the characteristic absorption peak of MNP at around 400 nm. Besides, the absorption peak at around 250 nm in the case of coke/Fe_3O_4 samples may be attributed to π–π^* transition for carbon materials [26]. The surface area values of coke/Fe_3O_4 composite samples (Table 1), especially prepared with coke samples of lowest particle size (C-62), were relatively higher than the values of either MNP

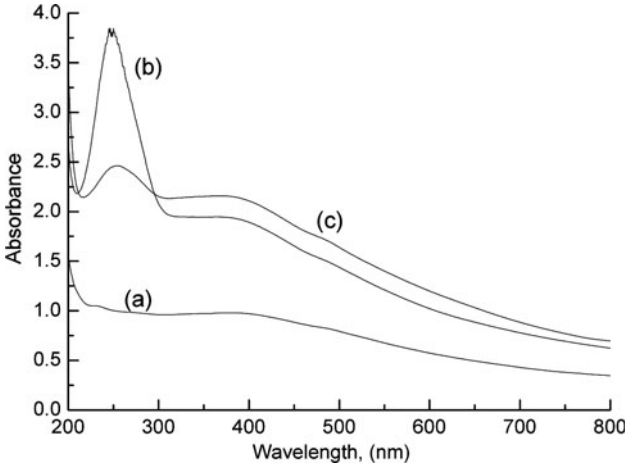

Fig. 2. UV–vis spectra of (a) neat MNP, (b) In-62 and (c) Ex-62.

or C-62. In comparison, the surface area of composite samples prepared *in situ* showed marginally higher surface area than those prepared by *ex situ* method.

The magnetization of MNP along with In-62 and Ex-62 samples at room temperature under variable-applied magnetic field was presented in Fig. 3. Both MNP and coke/Fe_3O_4 composites showed superparamagnetic behaviour (i.e. zero coercive field and zero remnant magnetization) most likely due to small size of the MNPs. Moreover, this behaviour would facilitate their easy recovery in a suspended system by an external magnetic field for repeated use. As evident from the figure, the value of magnetization decreased from the plateau value to zero, when the magnetic field was removed indicating the iron oxide particles correspond to the single-crystal domain exhibiting only one orientation of the magnetic moment. The value of saturation magnetization in case of MNP (22.51 emu g^{-1}) was much lower than bulk magnetite (σ_s = 92 emu g^{-1}), but comparable with those reported for similar sizes of MNP synthesized by different methods [27,28]. This value was decreased further in the cases of In-62 and Ex-62 (6.54 and 15.96 emu g^{-1}, respectively), obviously due to the contribution of non-magnetic component (i.e. coke) to the total sample mass as well as the small size of MNP [15,20].

The SEM micrographs of MNP and composite samples (In-62 and Ex-62) are presented in Fig. 4 along with their corresponding EDX. The presence of MNP and coke constituents was also evident from the corresponding EDX analyses (Fig. 4(d)–(f)). TEM micrograph (Fig. 5(a)) showed that MNP was well dispersed and nearly spherical in shape with particle sizes in the range 5–10 nm. The TEM of representative coke/MNP composites (Fig. 5(b) and (c)) showed a uniform distribution of MNP (black regions) on coke base (light grey region). The size of MNP in the composites matched reasonably well with the average particle size value obtained from XRD pattern. Aggregation of some Fe_3O_4 nanoparticles (marked with stars) was also seen owing to the magneto dipole interactions between the particles [11a].

It is well known that surface charge is one of the dominant factors in deciding the overall adsorption capacity of any adsorbent [11a]. Magnetite, an amphoteric solid, can develop positive and negative charges, respectively, due to protonation ($FeOH + H^+ \rightarrow FeOH_2^+$) and deprotonation ($FeOH \rightarrow FeO^- + H^+$) of FeOH sites generated on the surface of MNP or coke/Fe_3O_4 composites when dispersed in water. Hence, it is important to determine the point of zero charge (pH_{pzc}) of the samples, so that the nature of charge on their surface can be predicted at a given pH. The pH_{pzc} of neat MNP sample was found to be

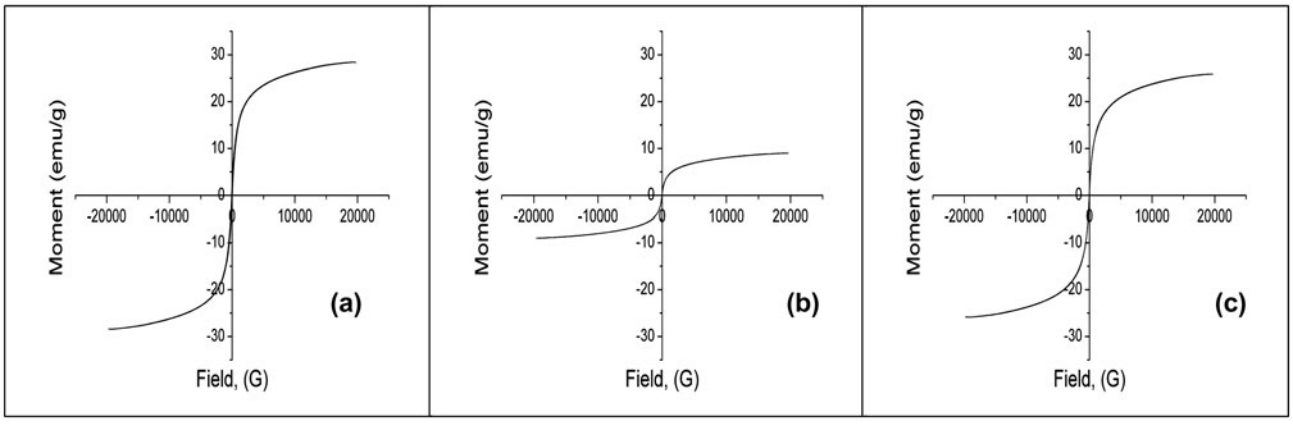

Fig. 3. Magnetization curves of (a) neat MNP, (b) In-62 and (c) Ex-62 at room temperature.

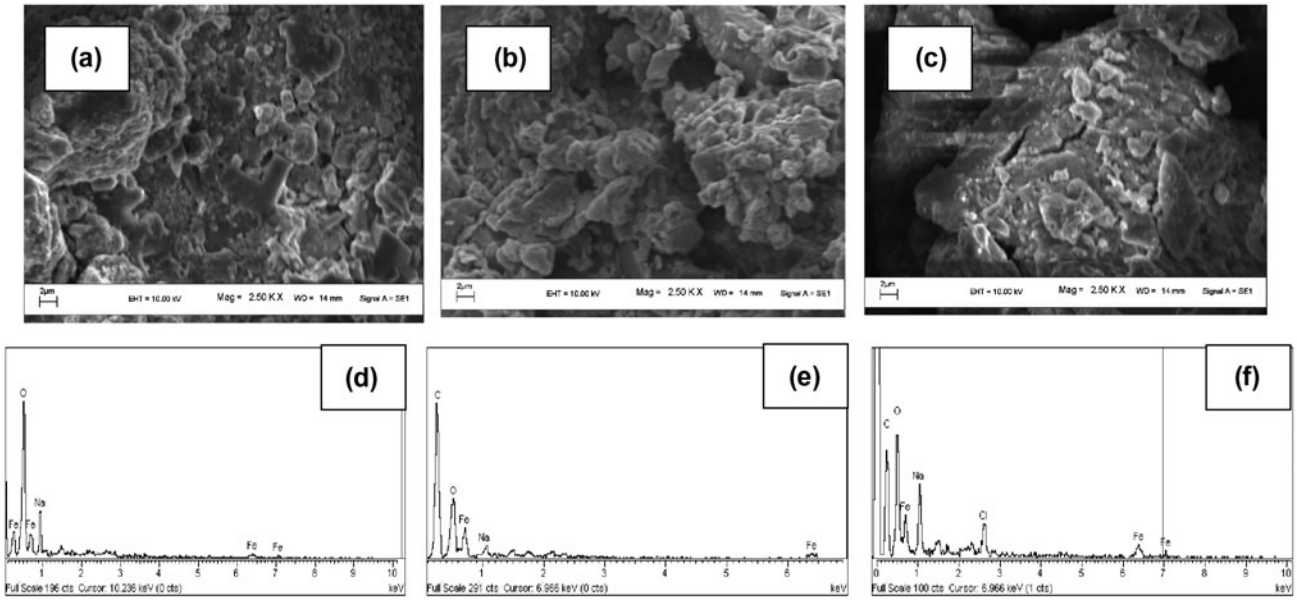

Fig. 4. SEM micrographs with EDX of (a and d) neat MNP, (b and e) In-62 and (c and f) Ex-62.

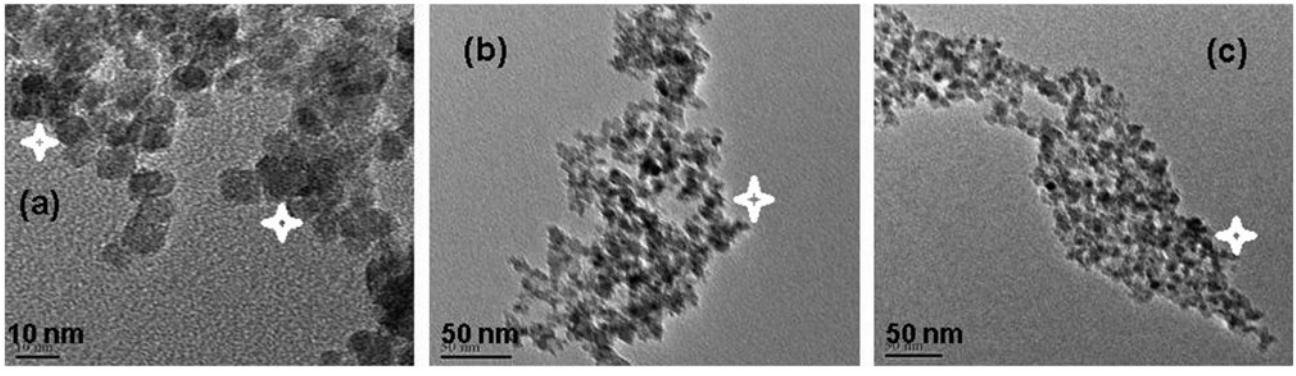

Fig. 5. TEM images of (a) neat MNP, (b) In-62 and (c) Ex-62.

7.2, while the same for coke/Fe_3O_4 composites is marginally lower and found in the range 6.8 ± 0.2. The lower pH_{pzc} value in the case of coke/Fe_3O_4 composites than neat MNP was presumably due to the presence of coke having a lower pH_{pzc} value (6.5 for C-62 coke sample). It may also be noted that the pH_{pzc} value of coke sample is quite close to that reported (≈6.6) for commercially activated charcoal [9]. The surface of coke/Fe_3O_4 composites would be either positively or negatively charged at pH <6.8 or >6.8, respectively, which entails the advantage of the removal of anionic or cationic contaminants from water via adsorption at different pH levels.

3.2. Adsorption behaviour of coke/Fe_3O_4 composites

3.2.1. Preliminary results

Preliminary results showed that the adsorption on neat MNP or coke/MNP composite was quite rapid and the adsorption equilibrium was reached within 10 min, regardless of the initial dye concentration as also observed in earlier studies [11a]. More than 90% adsorption of both dyes on coke/Fe_3O_4 composites occurred within 2–3 min followed by a slow process leading to equilibrium within 10 min. This was much lower than the time of adsorption equilibrium (180 min) for any of the coke sample when used alone. The faster rate of dye adsorption on MNP or coke/Fe_3O_4 composites primarily attributed to the absence of any internal diffusion and the adsorption occurred only on the surface of adsorbent and/or due to smaller size of the coke/Fe_3O_4 composites [6].

3.2.2. Effect of initial pH

The pH of the medium is a crucial parameter which influences the surface charge of adsorbent as well as its adsorption capacity. In order to avoid any variation of absorbance/colour change as a result of acid–base dissociation of dye molecules, the pH of the adsorbate solution was varied in between 4 and 10 for MB (pK_a ≈ >12) and 5 and 11 for CR (pK_a ≈ 3.0–5.0). The effects of varying pH on percentage adsorption of MB and CR at fixed concentration of dyes (10 mg L^{-1}) are shown in Figs. 6 and 7, respectively. It was evident that the adsorption of both dyes is strongly pH dependent showing an increase in MB adsorption or decrease in CR adsorption with an increase in the pH in the studied range. Similar trends have also been reported for the adsorption of cationic (MB) and anionic (CR) dye adsorption onto neat Fe_3O_4 [11a]. At lower pH, the positive surface charge of coke, Fe_3O_4 or coke/Fe_3O_4 composites facilitated the adsorption of

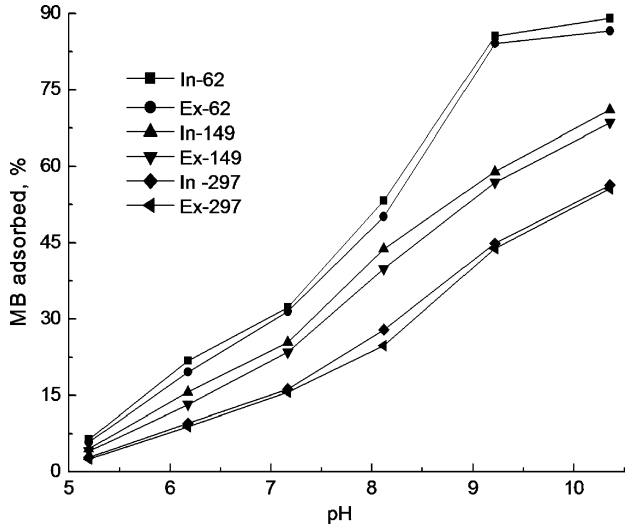

Fig. 6. Effect of pH on MB adsorption by coke/MNP composite samples (initial MB, 20 mg L^{-1} and adsorbent dose 1.0 g L^{-1}).

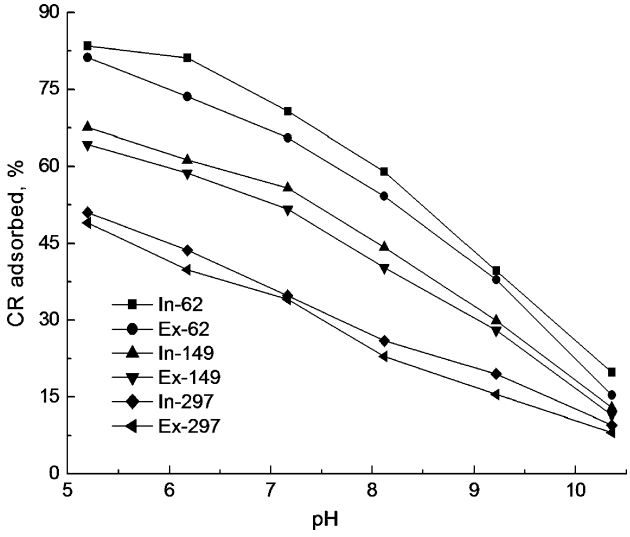

Fig. 7. Effect of pH on CR adsorption by coke/MNP composite samples (initial CR, 20 mg L^{-1} and adsorbent dose 1.0 g L^{-1}).

anionic dye while at pH above pH_{pzc} values (≥6.5), the surface of adsorbent gradually developed a higher negative charge leading to an increase in the cationic dye adsorption. Although the electrostatic interaction largely controlled the overall adsorption of dyes onto coke/Fe_3O_4 composites, significant amount of adsorption of MB and CR at pH below and above the pH_{pzc} values indicated that other adsorption mechanisms like complexation between surface active sites of MNP ($\equiv FeOH_2^+$/ $\equiv FeOH$/ $\equiv FeO^-$) and acid–base

functional groups of coke with dye molecules were also operative simultaneously. Based on the above, further optimization was carried out at pH ≈ 6.0 and 9.0 for CR and MB, respectively.

3.2.3. Effect of adsorbent mass

The variations of adsorbent (In-62 and Ex-62) dose in the range 0.5–4.0 g L^{-1} at fixed pH and initial dye concentration (20 mg L^{-1} for each MB/CR) showed a rapid increase up to 2.0 g L^{-1} and thereafter, non-linear but progressive increase was observed on further increase in the adsorbent dose. For instance, the percentage of MB adsorption increased from 61.2 to 94.5% with an increase in the adsorbent (In-62) dose 0.5–2.0 g L^{-1}, while an increase from 55.4 to 92.6% was observed in the case of CR for a similar increase in the adsorbent dose. Similar results have been reported previously for the adsorption of dyes on Fe_3O_4 nanoparticles and activated carbon [8,9,11a]. The non-linear increase in dye adsorption at higher dose was understandably due to the non-availability of enough adsorbate for adsorption. Hence, the amount of 1.0 g L^{-1} was chosen as an optimal adsorbent dose for further experiments.

3.2.4. Effect of initial dye concentration

Figs. 8 and 9 demonstrate the effect of varying initial dye concentrations (10–100 mg L^{-1}) on per cent adsorption of MB/CR at fixed adsorbent dose (1.0 g L^{-1}) and pH. As evident, the per cent adsorption of dyes decreased with an increase in the initial concentration in all the cases due to the fact that each adsorbent has a limited number of active sites which got saturated at a specific concentration. On the other hand, the amount of MR/CR adsorbed in each adsorbent was increased with an increase in the initial dye concentrations. For instance, the MB and CR uptakes increased from 9.11 to 47.85 mg g^{-1} and 9.42 to 56.19 mg g^{-1}, respectively, for In-62 composite with an increase in the dye concentration from 10 to 100 mg L^{-1}. The equilibrium adsorption data at varying initial dye concentrations were further analysed with the well-known Langmuir and Freundlich isotherms. The linear form of Langmuir and Freundlich isotherms was given by Eqs. (3) and (4), respectively.

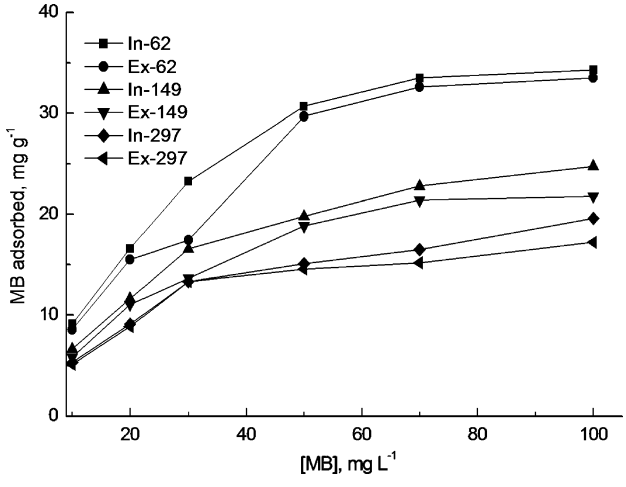

Fig. 8. Effect of initial MB concentration on its adsorption by coke/MNP composite samples at pH ≈ 9.0 ± 0.2 with adsorbent dose 1.0 g L^{-1}.

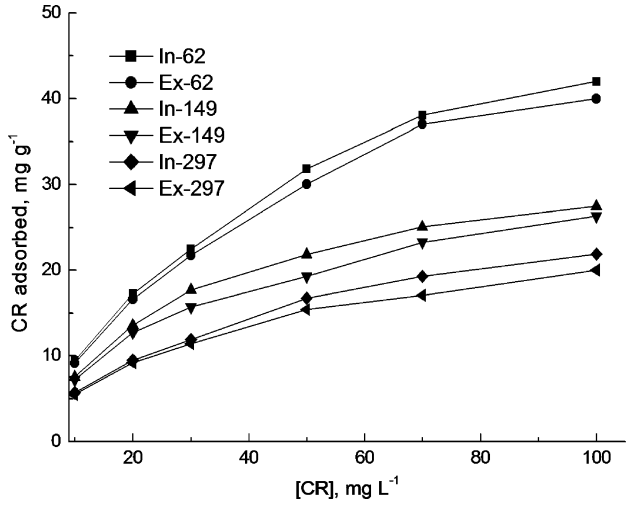

Fig. 9. Effect of initial CR concentration on its adsorption of CR by coke/MNP composite samples at pH ≈ 6.0 ± 0.2 with adsorbent dose 1.0 g L^{-1}.

$$C_e/q_e = 1/bQ_0 + C_e/Q_0 \quad (3)$$

$$\log q_e = 1/n(\log C_e) + \log K \quad (4)$$

where C_e (mg L^{-1}) is the equilibrium dye concentration in solution, q_e (mg g^{-1}) is the equilibrium MB or CR uptake per unit mass of adsorbent, Q_0 (mg g^{-1}) is the maximum adsorption capacity and b (L mg^{-1}) is the Langmuir constant and related to the energy of adsorption, K and $1/n$ are roughly the indicators of adsorption capacity of the Freundlich constants and considered to be relative indicators of adsorption capacity (L g^{-1}) and adsorption intensity, respectively.

The adsorption parameters derived from the least square fittings of adsorption data to the linearized form of the Langmuir and Freundlich equations are

Table 2
Adsorption parameters derived from the Langmuir and Freundlich isotherms for the adsorption of MB/CR on MNP-AC nanocomposite and other relevant materials

Sample description	Dye	Initial [dye] (mg L^{-1})	pH	Langmuir			Freundlich			Refs.
				Q_0 (mg g^{-1})	b (L mg^{-1})	R^2	K (L g^{-1})	n	R^2	
MNP	MB	1.6–32	9.4	70.4	0.229	0.989	6.660	1.481	0.998	[11a]
	CR	10.45–55.73	6.2	172.41	0.153	0.985	40.364	2.645	0.994	
Maghemite nanoparticles	CR	–	5.9	208.33	–	–	–	–	–	[29]
PAA bound MNP	MB	50–800	9.0	199	–			–		[30]
Magnetite powder	MB	1.6–32	9.21	20.74	0.051	0.968	1.284	1.361	0.990	[31]
AC (date pits/modified)	CR	~50–800	5.5–6.5	61–105	0.009–0.0133	0.95–99	5–8.1	2.3–2.6	0.92–0.96	[32]
AC (commercial)	CR	50–545	7.0	300	6.49×10^{-3}	0.94	20.7	2.7	0.97	[9]
Coke (500–900°C)[a]	MB	1–12	7.2	24.9–58.9	0.42–2.59	0.998	91.2–238	0.994	0.994	[24]
Coke (hard/soft coal)	MB	10–100	8.0	13.5		0.996				[25]
	CR									
Mesoporous carbon/MNP	MB	–		608.04		–	–			[34]
	CR	–	–	1,656.9		–	–			
Graphene/magnetite	MB	–		43.82	0.2946		16.56	3.452	0.753	[15]
In-62	CR	10–100	6.0[b]	44.84	0.192	0.996	6.16×10^{-4}	0.333	0.992	This work
Ex-62	CR	10–100	6.0	43.49	0.163	0.992	1.62×10^{-3}	0.359	0.989	This work
In-149	CR	10–100	6.0	30.30	0.115	0.998	0.015	0.389	0.954	This work
Ex-149	CR	10–100	6.0	29.41	0.088	0.988	0.015	0.390	0.975	This work
In-297	CR	10–100	6.0	27.02	0.051	0.993	0.103	0.476	0.990	This work
Ex-297	CR	10–100	6.0	25.58	0.043	0.991	0.316	0.569	0.931	This work
In-62	MB	10–100	9.0[b]	37.49	0.247	0.997	$9.36 \times 1\ 0^{-4}$	0.332	0.965	This work
Ex-62	MB	10–100	9.0	36.32	0.185	0.999	4.66×10^{-3}	0.389	0.954	This work
In-149	MB	10–100	9.0	29.23	0.072	0.993	0.039	0.439	0.976	This work
Ex-149	MB	10–100	9.0	28.32	0.063	0.994	0.136	0.538	0.964	This work
In-297	MB	10–100	9.0	23.04	0.058	0.993	0.099	0.456	0.971	This work
Ex-297	MB	10–100	9.0	19.96	0.069	0.997	0.100	0.442	0.953	This work

[a]Lignite pyrolysis temperature.
[b]pH values vary within ±0.2.

given in Table 2 along with the same reported for other relevant adsorbents. A slightly better fitting of adsorption data to the Freundlich isotherm indicated the heterogeneous surface of adsorbent. As expected, the derived monolayer capacities (Q_0) for both the dyes were decreased with an increase in the coke size of the coke/Fe_3O_4 composite sample primarily due to the lower surface area and surface active sites. Further, Q_0 values of different coke/Fe_3O_4 composites for MB (19.9–36.3 mg g^{-1}) or CR (25.6–44.8 mg g^{-1}) were relatively lower than those observed for neat magnetite/maghemite nanoparticles [11a,29] or coated MNPs [30] partly due to the lower MNP content in the coke/Fe_3O_4 composites. The Q_0 values for MB adsorption were, however, comparable or higher with the same obtained with the magnetite powder of relatively larger size [31]. In comparison to the activated carbon or charcoal, whose adsorption capacities are widely varied depending on the starting materials, preparation methods and experimental conditions [9,32], the adsorption capacities of the coke/Fe_3O_4 are expected to be lower because of their relatively low surface area (see Table 2). In some cases, however, the Q_0 values were even comparable or higher. For instance, the adsorption capacity of AC from coir pith for CR was reported very low (6.72 mg g^{-1}) in the concentration range (20–80 mg L^{-1}) [33]. It was also worth noting that the adsorption capacities of coke/MNP composites towards MB were comparable with the same reported for coke derived from lignite [24], but higher than those obtained from coke sample derived from the pyrolysis of hard/soft-coal blending [25] (see Table 2). This clearly indicated that the presence of MNP in the coke/MNP composites was primarily responsible for enhancing the adsorption efficiency. Since there is no report on adsorption of dyes using magnetic coke, it is worthwhile to compare the adsorption parameters with those reported for some carbonaceous materials/magnetite composites [15,34]. On one hand, the values of adsorption capacity for both the dyes were much lower than those reported (Table 2) with mesoporous carbon/MNP composite due to significantly higher porosity in the case of latter, while the Q_0 value, reported (43.82 mg g^{-1}) for MB in the case of graphene/magnetite nanocomposites [15], was more or less comparable with the values obtained in the present case. The above observations indicated that the nature of carbonaceous materials greatly influences the overall adsorption efficiency of composite samples for different dyes. Among MB and CR, the monolayer adsorption capacity of coke/Fe_3O_4 composite samples was invariably found higher for CR than that observed for MB under identical conditions, presumably due to more favourable electrostatic interaction of anionic dye with coke/Fe_3O_4 composites. Relatively higher adsorption of anionic dye (e.g. CR) on MNP or MNP-based composites with carbonaceous materials over cationic dyes (e.g. MB) has also been reported in the previous studies [11a,25].

3.2.5. Desorption study

In order to explore the potential of coke/Fe_3O_4 composites for repeated use, desorption of dyes adsorbed on the adsorbent was studied. As the adsorption of dyes was dependent on the pH of the adsorbing media, it was thought that the desorption of MB/CR is possible by controlling the pH of the eluent. As such, the desorption of MB/CR from MB/CR-loaded adsorbents was initially carried out using water at varying pH (5.0–11.0) as the eluent. On shaking of the CR-loaded composite at pH ≈ 9.0 for 5 min, 93.5% of adsorbed CR gets desorbed and almost complete desorption was achieved at pH ≈ 12.0. On the other hand, only a small amount of MB (≈6.7%) got desorbed at pH < 7.0. However, the extent of desorption of MB was greatly enhanced using a methanolic solution of acetic acid as the eluent which increased with an increase in the acetic acid content of methanol and more than 89% of MB was desorbed with 6% (v/v) acetic acid in methanol. Similar observation was made previously in the case of dye desorption from magnetite [11a,35]. The fast desorption equilibrium (within 5 min) similar to that of adsorption also indicated the absence of internal diffusion resistance in the coke/Fe_3O_4 composites. Further study is required to optimize the conditions for surface modification and regeneration of coke/Fe_3O_4 composites for its possible large-scale applications in the treatment of wastewaters.

4. Conclusions

In conclusion, the present study demonstrated a simple route of preparing coke/Fe_3O_4 composites using the coke derived from industrial grade coking coals and Fe_3O_4 nanoparticles prepared using waste IOTs as one of the starting materials. The resulted composites, characterized by PXRD, UV–vis–DRS coupled with SEM–EDX and TEM, revealed more or less uniform distribution of nearly spherical MNPs. The obtained composites showed superparamagnetic characteristic which allowed them to be easily manipulated by an external magnetic field. All the composite samples were found efficient for the fast removal of organic dyes like MB and CR from their aqueous solutions and efficiency was dependent on

several factors like pH, initial dye concentration and adsorbent dose. The equilibrium adsorption data were better fitted to the Freundlich isotherm model. The desorption of CR from coke/Fe_3O_4 composites was strongly pH dependent and almost compete desorption of adsorbed CR was achieved at pH ≈ 12.0, while desorption of MB was much lower under identical conditions. Moreover, the present set of data may be helpful in designing a promising low-cost adsorbent for the removal of organic compounds including dyes from industrial wastewater.

References

[1] V.K. Gupta, P.J.M. Carrott, M.M.L. Ribeiro Carrott, Suhas, Low-cost adsorbents: Growing approach to wastewater treatment—A review, Crit. Rev. Environ. Sci. Technol. 39 (2009) 783–842.

[2] V.K. Gupta, Suhas, Application of low-cost adsorbents for dye removal—A review, J. Environ. Manage. 90 (2009) 2313–2342.

[3] S.H. Lin, R.S. Juang, Adsorption of phenol and its derivatives from water using synthetic resins and low-cost natural adsorbents: A review, J. Environ. Manage. 90 (2009) 1336–1349.

[4] S.K. Reddy Yadanaparthi, D. Graybill, R. von Wandruszka, Adsorbents for the removal of arsenic, cadmium, and lead from contaminated waters, J. Hazard. Mater. 171 (2009) 1–15.

[5] D. Mohan, C.U. Pittman Jr., Activated carbons and low cost adsorbents for remediation of tri- and hexavalent chromium from water, J. Hazard. Mater. 137 (2006) 762–811.

[6] J. Rivera-Utrilla, M. Sánchez-Polo, V. Gómez-Serrano, P.M. Álvarez, M.C.M. Alvim-Ferraz, J.M. Dias, Activated carbon modifications to enhance its water treatment applications. An overview, J. Hazard. Mater. 187 (2011) 1–23.

[7] B. Petrova, T. Budinova, B. Tsyntsarski, V. Kochkodan, Z. Shkavro, N. Petrov, Removal of aromatic hydrocarbons from water by activated carbon from apricot stones, Chem. Eng. J. 165 (2010) 258–264.

[8] M.F.R. Pereira, S.F. Soares, J.J.M. Órfão, J.L. Figueiredo, Adsorption of dyes on activated carbons: Influence of surface chemical groups, Carbon 41 (2003) 811–821.

[9] M.K. Purkait, A. Maiti, S. DasGupta, S. De, Removal of congo red using activated carbon and its regeneration, J. Hazard. Mater. 145 (2007) 287–295.

[10] R.D. Ambashta, M. Sillanpää, Water purification using magnetic assistance: A review, J. Hazard. Mater. 180 (2010) 38–49.

[11] (a) S.K. Giri, N.N. Das, G.C. Pradhan, Synthesis and characterization of magnetite nanoparticles using waste iron ore tailings for adsorptive removal of dyes from aqueous solution, Colloids Surf., A 389 (2011) 43–49; (b) G.R. Chaudhary, P. Saharan, A. Kumar, S.K. Mehta, S. Mor, A. Umar, Adsorption studies of cationic, anionic and azo-dyes via monodispersed Fe_3O_4 nanoparticles, J. Nanosci. Nanotechnol. 13 (2013) 3240–3245; (c) G.R. Chaudhary, P. Saharan, S.K. Mehta, S. Mor, A. Umar, Fast and efficient removal of hazardous Congo red from its aqueous solution using Fe_2O_3 nanoparticles, J. Nanoeng. Nanomanuf. 3 (2013) 142–146; (d) P. Saharan, G.R. Chaudhary, S.K. Mehta, A. Umar, Removal of water contaminants by iron oxide nanomaterials, J. Nanosci. Nanotechnol. 14 (2014) 627–643.

[12] D. Mohan, A. Sarswat, V.K. Singh, M. Alexandre-Franco, C.U. Pittman Jr., Development of magnetic activated carbon from almond shells for trinitrophenol removal from water, Chem. Eng. J. 172 (2011) 1111–1125.

[13] I. Safarik, K. Horska, K. Pospiskova, M. Safarikova, Magnetically responsive activated carbons for bio- and environmental applications, Int. Rev. Chem. Eng. 4 (2012) 346–352.

[14] G. Zhang, J. Qu, H. Liu, A.T. Cooper, R. Wu, $CuFe_2O_4$/activated carbon composite: A novel magnetic adsorbent for the removal of acid orange II and catalytic regeneration, Chemosphere 68 (2007) 1058–1066.

[15] L. Ai, C. Zhang, Z. Chen, Removal of methylene blue from aqueous solution by a solvothermal-synthesized graphene/magnetite composite, J. Hazard. Mater. 192 (2011) 1515–1524.

[16] S.R. Rudge, T.L. Kurtz, C.R. Vessely, L.G. Catterall, D.L. Williamson, Preparation, characterization, and performance of magnetic iron–carbon composite microparticles for chemotherapy, Biomaterials 21 (2000) 1411–1420.

[17] A.B. Fuertes, P. Tartaj, A facile route for the preparation of superparamagnetic porous carbons, Chem. Mater. 18 (2006) 1675–1679.

[18] N. Yang, Sh. Zhu, D. Zhang, Sh. Xu, Synthesis and properties of magnetic Fe_3O_4-activated carbon nanocomposite particles for dye removal, Mater. Lett. 62 (2008) 645–647.

[19] C.S. Castro, M.C. Guerreiro, M. Gonçalves, L.C.A. Oliveira, A.S. Anastácio, Activated carbon/iron oxide composites for the removal of atrazine from aqueous medium, J. Hazard. Mater. 164 (2009) 609–614.

[20] M.H. Do, N.H. Phan, T.D. Nguyen, T.T.S. Pham, V.K. Nguyen, T.T.T. Vu, T.K.P. Nguyen, Activated carbon/Fe_3O_4 nanoparticle composite: Fabrication, methyl orange removal and regeneration by hydrogen peroxide, Chemosphere 85 (2011) 1269–1276.

[21] B. Kakavandi, A.J. Jafari, R.R. Kalantary, S. Nasseri, A. Ameri, A. Esrafily, Synthesis and properties of Fe_3O_4-activated carbon magnetic nanoparticles for removal of aniline from aqueous solution: Equilibrium, kinetic and thermodynamic studies, Iran. J. Environ. Health Sci. Eng. 10 (2013) 1–9.

[22] Y. Zhang, S. Xu, Y. Luo, S. Pan, H. Ding, G. Li, Synthesis of mesoporous carbon capsules encapsulated with magnetite nanoparticles and their application in wastewater treatment, J. Mater. Chem. 21 (2011) 3664–3671.

[23] S. Ilday, Z. Mısırlıoğlu, M. Canel, A. Sınağ, Removal of methylene blue from aqueous media by using cokes obtained from lignite pyrolysis, Energy Sources Part A 36 (2014) 2183–2193.

[24] P. Hu, Y. Zhang, K. Tong, F. Wei, Q. An, X. Wang, P.K. Chu, F. Lv, Removal of organic pollutants from red water by magnetic-activated coke, Desalin. Water Treat. 54 (2105) 2710–2722.
[25] P. Sahoo, R. Das, N.N. Das, Adsorptive removal of aqueous phenol using coke derived from hard/soft coking coal blends, Environ. Technol. (communicated).
[26] C. Jäger, T.H. Henning, R. Schlögl, O. Spillecke, Spectral properties of carbon black, J. Non-Cryst. Solids 258 (1999) 161.
[27] F. Yazdani, M. Edrissi, Effect of pressure on the size of magnetite nanoparticles in the coprecipitation synthesis, Mater. Sci. Eng.: B 171 (2010) 86–89.
[28] W. Pei, H. Kumada, T. Natusme, H. Saito, S. Ishio, Study on magnetite nanoparticles synthesized by chemical method, J. Magn. Magn. Mater. 310 (2007) 2375–2377.
[29] S.Y. Mak, D.H. Chen, Fast adsorption of methylene blue on polyacrylic acid-bound iron oxide magnetic nanoparticles, Dyes Pigm. 61 (2004) 93–98.
[30] A. Afkhami, R. Moosavi, Adsorptive removal of Congo red, a carcinogenic textile dye, from aqueous solutions by maghemite nanoparticles, J. Hazard. Mater. 174 (2010) 398–403.
[31] S.K. Giri, N.N. Das, G.C. Pradhan, Magnetite powder and kaolinite derived from waste iron ore tailings for environmental applications, Powder Technol. 214 (2011) 513–518.
[32] M. Belhachemi, F. Addoun, Adsorption of congo red onto activated carbons having different surface properties: Studies of kinetics and adsorption equilibrium, Desalin. Water Treat. 37 (2012) 122–129.
[33] C. Namasivayam, D. Kavitha, Removal of congo red from water by adsorption onto activated carbon prepared from coir pith, an agricultural solid waste, Dyes Pigm. 54 (2002) 47–58.
[34] Y. Zhang, S. Xu, Y. Luo, S. Pan, H. Ding, G. Li, Synthesis of mesoporous carbon capsules encapsulated with magnetite nanoparticles and their application in wastewater treatment, J. Mater. Chem. 21 (2011) 3664–3671.
[35] I. Šafařík, Removal of organic polycyclic compounds from water solutions with a magnetic chitosan based sorbent bearing copper phthalocyanine dye, Water Res. 29 (1995) 101–105.